High-speed particle tracking in microscopy using SPAD image sensors

High-speed particle tracking in microscopy using SPAD image sensors

Istvan Gyongy*[a], Amy Davies*[b], Allende Miguelez Crespo[b], Andrew Green[b], Neale A.W. Dutton[c], Rory R. Duncan[b], Colin Rickman[b], Robert K. Henderson[a], Paul A. Dalgarno[b]
[a]Institute for Integrated Micro and Nano Systems, School of Engineering, University of Edinburgh, Edinburgh EH9 3JL, UK; [b]Institute of Biological Chemistry, Biophysics and Bioengineering, School of Engineering & Physical Science, Heriot-Watt University, Edinburgh EH14 5AS, UK; [c]Imaging Division, STMicroelectronics, Edinburgh EH3 5DA, UK

ABSTRACT

Single photon avalanche diodes (SPADs) are used in a wide range of applications, from fluorescence lifetime imaging microscopy (FLIM) to time-of-flight (ToF) 3D imaging. SPAD arrays are becoming increasingly established, combining the unique properties of SPADs with widefield camera configurations. Traditionally, the photosensitive area (fill factor) of SPAD arrays has been limited by the in-pixel digital electronics. However, recent designs have demonstrated that by replacing the complex digital pixel logic with simple binary pixels and external frame summation, the fill factor can be increased considerably. A significant advantage of such binary SPAD arrays is the high frame rates offered by the sensors (>100kFPS), which opens up new possibilities for capturing ultra-fast temporal dynamics in, for example, life science cellular imaging. In this work we consider the use of novel binary SPAD arrays in high-speed particle tracking in microscopy. We demonstrate the tracking of fluorescent microspheres undergoing Brownian motion, and in intra-cellular vesicle dynamics, at high frame rates. We thereby show how binary SPAD arrays can offer an important advance in live cell imaging in such fields as intercellular communication, cell trafficking and cell signaling.

Keywords: Particle tracking, Single-photon avalanche diode, Photon counting image sensor, Fluorescence microscopy

1. INTRODUCTION

Single photon avalanche diodes are a well-established technology in biomedical imaging, especially in Fluorescence Lifetime Imaging Microscopy (FLIM) applications [1], which exploit the single-photon sensitivity and picosecond time resolution of SPAD devices. Traditionally, SPAD sensors in microscopy have been single-point detectors (necessitating optical scanning apparatus), but technological advances such as compact, analogue pixels [2], stacked, back-side illuminated (BSI) architectures [3], as microlensing [4], are now yielding photon-counting image sensors with increasing spatial resolution and fill factors for widefield applications.

Whilst the quantum efficiency (QE) of these sensors still lags behind EMCCD and sCMOS cameras, very high frame rates are possible, particularly in binary SPAD sensors, which can provide frame rates in excess of 100kFPS [5]. Crucially, as readout noise is negligible, the raw output of binary fields (or "bit-planes"), and individual photon detections therein, can be summed to compose higher bit-depth images without any noise penalty. Indeed, by tailoring the summation to specific applications, useful advantages have been demonstrated, such as reduced motion blur when imaging high-speed objects [6], the reconstruction of moving objects in low-light conditions [7], and improved background rejection in single molecule localisation microscopy [8], leading to localisation performance comparable to an EMCCD.

In the specific context of particle tracking, the flexibility in composing images from bit-planes allows the effective frame rate to be set in post-processing (based on the level of bit-plane aggregation). Thus, the same data set may be analysed at different frame rates, enabling post-acquisition optimisation for particular brightness and speed of particles. This paper considers two exemplar examples of particle tracking with a SPAD device: the tracking of fluorescent microspheres undergoing Brownian motion, and fluorescently-labelled cell vesicles. We present experimental results obtained with a 320×240, >10kfps SPAD camera [2], which is one of the highest resolution SPAD imagers available, and also has one of the highest fill-factors at 50% (after microlensing [9]).

*Equal authors: istvan.gyongy@ed.ac.uk, amy.davies@hw.ac.uk

2. TRACKING OF BROWNIAN MOTION

2.1 Simulation study

To gain an understanding of the limits of particle tracking using a high-frame rate binary SPAD sensor, a simulation model was created. The model, representing a 64×64 detector array, simulates the imaging of a single particle with Brownian motion, based on a certain background B and particle photon rate I and uses a diffraction-limited point spread function (PSF) modelled by a 2D Gaussian function with sigma=1.5. Between every bit-plane, the particle position is moved by random steps Δx_i, Δy_i, drawn from independent normal distributions with mean zero and standard deviation $\sqrt{(2Dt)}$ [10], where D is the diffusion coefficient and t is the time interval between bit-planes. The SPAD bit-planes are synthesised according to Poisson statistics given the prescribed B, I, and the current location of the particle PSF, and image frames are then generated by summing bit-planes in non-overlapping groups of N.

The resulting synthesised image data set (based on 1000 generated tracks for every different N) were then tracked using gaussMLE [11], to extract trajectories and motion statistics. A standard metric for assessing particle trajectories in microscopy is the mean square displacement (MSD), or its square root (RMSD) [12]. When plotted against the time interval between frames, it can reveal whether the observed motion is diffusion-dominated (i.e. random, as in this example), directed, or spatially constrained. It also allows the measurement error to be assessed. Figure 1 plots the RMSD, as a function of the level of aggregation N, for two different values of D. At large values of N, the tracking results can be seen to follow the true RMSD curve (given by $\sqrt{4Dt}$). However, as N is reduced, the measured RMSD bottoms out and then starts to increase again. This is a well-studied phenomenon [13], and is caused by the localisation error (due to the inherent photon noise in low photon count images) starting to dominate the RMSD. For a fixed I, the faster the particles are (the higher D is), the lower N one can go down to before encountering this effect. In practice, there is no benefit in choosing an N below the minimum in the RMSD curve, as no additional spatio-temporal information is obtained beyond that point.

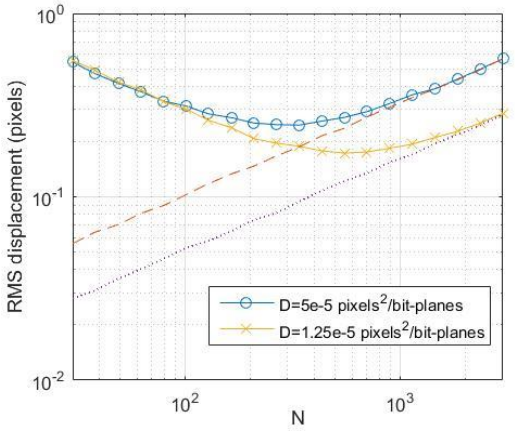

Figure 1. Simulation results for Brownian motion tracking with a binary SPAD, showing the measured RMSD as a function of bit-plane for two different (normalised) diffusion coefficients. The dashed and dotted lines represent the true RMSD in the two cases. A mean background photon rate of B=0.001 photons/bit-plane is specified, together with a mean photon rate of I=1 photon/bit-plane from the particle.

2.2 Experimental results

The simulation work was followed by experiments on a standard 60X widefield fluorescence microscope (Olympus IX71), in which microsphere samples were imaged using the SPAD camera operated at 20kfps. Sequences of image frames were created using different levels N of bit-plane aggregation (and background subtraction, as detailed in [8]), then analysed using TrackMate [14]. Figure 2 shows the results for a sample of 0.5μ red beads in a 50:50 mixture of glycerol and water. The RMSD is plotted for a single bead trajectory, as a function of the bit-plane aggregation (or total frame time). The shape of the curve corresponds well with the simulation results of Figure 1, and suggests that below 5ms (100 bit-plane) aggregation, localisation error from photon noise already starts to affect the measured frame-to-frame displacements. This is a consequence of underlying the diffusion process being relatively slow compared to the high frame rate of the camera.

In a practice, particles within a sample may exhibit different speeds and levels of brightness, so one can envisage analysing each trajectory individually (for different N), so as to optimise the spatio-temporal resolution in each case.

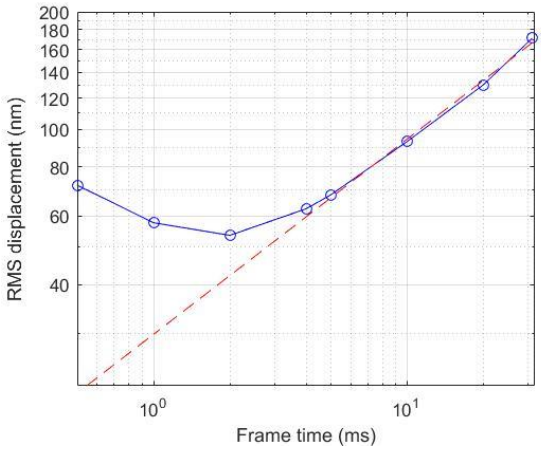

Figure 2. Plot of RMSD for microsphere sample, as a function of the frame time, on logarithmic axes. At higher frame times, the curve follows a straight line (as indicated by the dashed line), as expected from Brownian motion theory.

3. LIVE CELL VESICLE TRACKING

For the vesicle tracking experiments, large dense-core vesicles in secretory cells (Pheochromocytoma cells, PC12s) were labeled using soluble cargo Neuropeptide Y (NPY) fused to mCherry, as previously described [15]. To examine the mobility of vesicles, image sequences were acquired at 23°C under TIRF illumination using a 561nm excitation laser. An Olympus Cell Excellence IX81 microscope, with a 150× TIRF objective, was used, with all emission light directed to either an EMCCD camera (Hamamatsu ImageEM, with 30ms exposure, and 55ms frame time) or the SPAD camera (100µs exposure per bit-plane). The resultant SPAD bit-planes were subject to background subtraction and image frames were generated by summing bit-planes in groups of *N*. The EMCCD and SPAD imager frames were then analysed using TrackMate to extract particle tracks.

Figure 3 shows sample tracks obtained from the SPAD image frames for a given cell, for levels of aggregation of *N*=50, 100 and 550 (resulting in frame times of 5ms, 10ms and 55ms, respectively). Some vesicles appear to be constrained to specific positions in the cell, but longer tracks can also be seen, as expected [16]. The statistics of the tracks, together with those obtained from the EMCCD frames are given in Figure 4 (the EMCDD results are for an identically prepared cell, shown in Figure 5). The results are presented in the form of a histogram of the mean track speeds, a scatter plot of the maximum displacement (from initial position) vs total length of individual tracks, and an angle histogram plot (or rose plot) of the angle between successive steps (displacements) in the tracks. Comparing the EMCCD results (panel A) to those of the SPAD at equivalent frame time (panel B), we see broadly similar distributions of mean track speed (with mean value of 4.41µm/s for the EMCCD vs 4.33µm/s versus the SPAD), with both rose plots showing a clear directionality in the tracks (that would be absent from pure Brownian motion). The corresponding RMSD values are 0.076µm for the EMCCD versus 0.106µm for the SPAD. We note that as the frame time of the SPAD is reduced (to 10ms in panel C and 5ms in panel D), the directionality in the tracks becomes less pronounced. Indeed, the corresponding RMSD values of 0.086 µm and 0.089µm suggest that a minimum similar to those seen in Figures 1 and 2 has been reached, with the estimated tracks being impacted by photon noise.

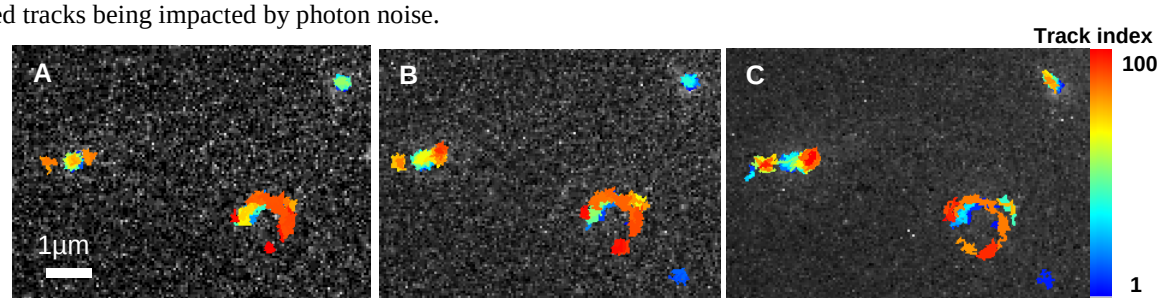

Figure 3. Vesicle tracks, superimposed on single image frames (a 150×110 ROI is shown), for different levels of bit-plane aggregation: (a) *N*=50, 5ms frame time, (b) *N*=100, 10ms frame time, (c) *N*=550, 55ms frame time.

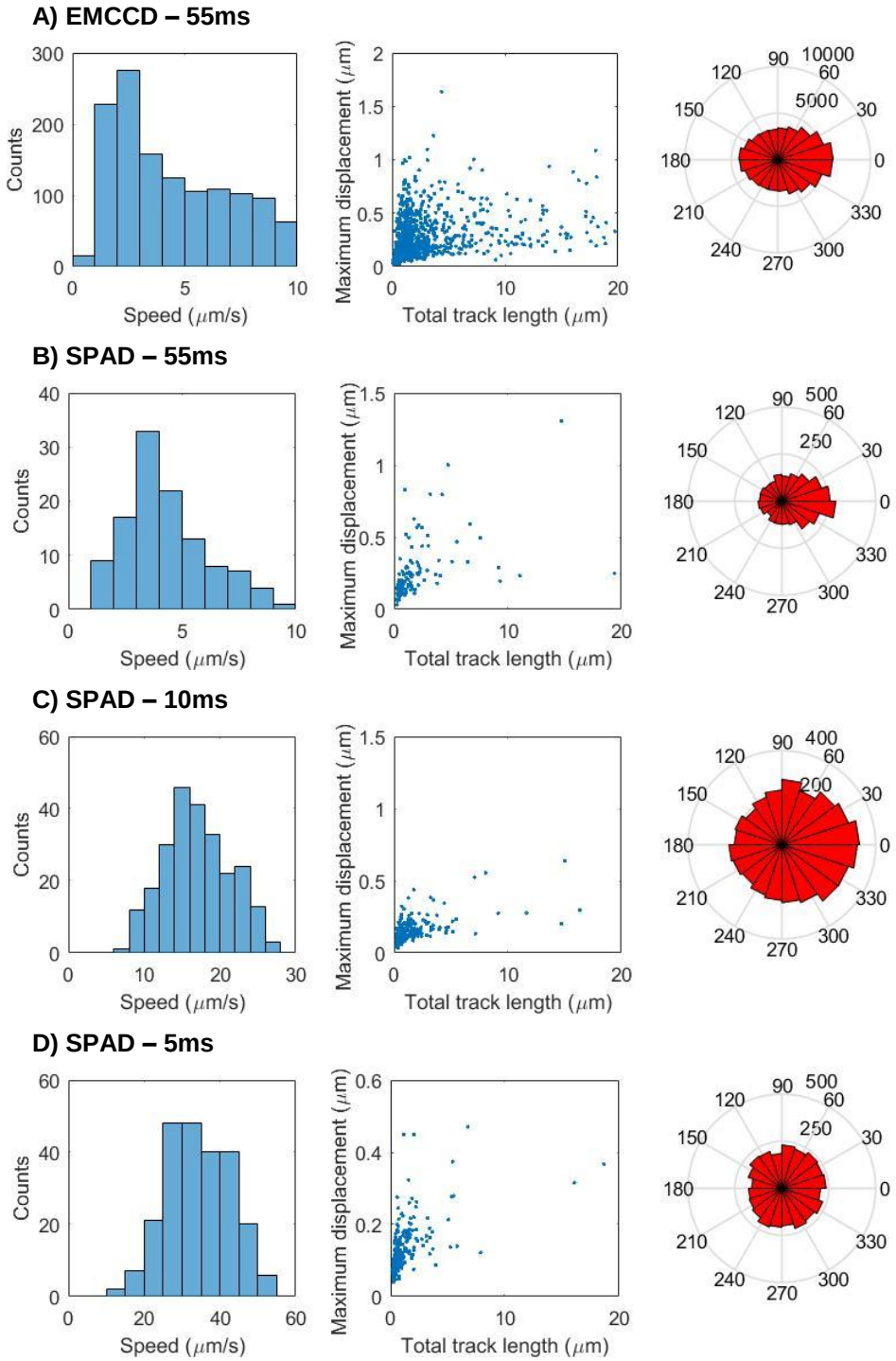

Figure 4. Vesicle tracking statistics, in terms of the histogram of mean track speed, scatter plot of maximum displacement versus track length, and polar histogram of relative angles between consecutive steps for (a) EMCCD (55ms frame time), (b) SPAD (55ms frame time), (c) SPAD (10ms frame time), (d) SPAD (5ms frame time). The EMCCD tracking results feature a considerably higher number of track segments (84083 vs 4638 for SPAD with 55ms frame time). This may be in in part due to the different cells in question, but also the higher inherent sensitivity (or quantum efficiency) of the EMCCD.

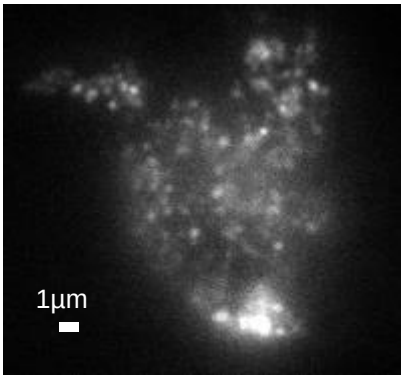

Figure 5. Image of secretory cells taken with EMCCD (30ms exposure time).

4. CONCLUSIONS

We have presented results from the application of a binary SPAD to high speed tracking of microspheres and cell vesicles, demonstrating the advantage of the frame rate being adjustable in post-processing, and thus optimisable to the imaging conditions, and even for individual tracks, so as to get the best possible spatio-temporal resolution, typically only limited by photon shot noise.

ACKNOWLEDGMENTS

This research was funded by the European Research Council (ERC) through the EU's Seventh Framework Programme (FP/2007-2013)/ERC under Grant 339747. The authors appreciate the support of STMicroelectronics who fabricated the chip. The use of the ESRIC facilities at Heriot-Watt University is also gratefully acknowledged.

REFERENCES

[1] Poland, S.P, Krstajić, N., Monypenny, J., Coelho, S., Tyndall, D., Walker, R.J., Devauges, V., Richardson, J., Dutton, N., Barber, P., and Li, D.D.U, "A high speed multifocal multiphoton fluorescence lifetime imaging microscope for live-cell FRET imaging," Biomed. Opt. Express 6(2), 277-296 (2015).

[2] Dutton, N.A.W., Parmesan, L., Holmes, A.J., Grant, L.A., and Henderson, R.K.,"320×240 oversampled digital single photon counting image sensor," Proc. IEEE VLSI Circuits Symposium, 1-2 (2014).

[3] Al Abbas, T., Dutton, N.A.W., Almer, O., Pellegrini, S., Henrion, Y., and Henderson, R.K., "Backside illuminated SPAD image sensor with 7.83µm pitch in 3D-stacked CMOS technology," Proc. IEDM, paper 8-1 (2016)

[4] Pavia, J.M., Wolf, M., and Charbon, E., "Measurement and modeling of microlenses fabricated on single-photon avalanche diode arrays for fill factor recovery," Opt. Express 22(4), 4202–4213 (2014).

[5] Antolovic, I.M., Burri, S., Bruschini, C., Hoebe, R., and Charbon, E., "Nonuniformity Analysis of a 65-kpixel CMOS SPAD Imager," IEEE Trans. Electron Devices 63(1), 57-64 (2016).

[6] Gyongy, I., Dutton, N.A.W., Davies, A., Saleeb, R., Duncan, R., Rickman, C., Dalgarno, P., and Henderson, R.K., "Bit-plane Processing Techniques for Low-Light, High Speed Imaging with a SPAD-based QIS," Proc. IISW (2015).

[7] Gyongy, I., Al Abbas, T., Dutton, N.A.W., and Henderson, R.K., "Object Tracking and Reconstruction with a Quanta Image Sensor," Proc. IISW, 242-245 (2017).

[8] Gyongy, I., Davies, A., Dutton, N.A.W., Duncan, R., Rickman, C., Henderson, R.K., and Dalgarno, P., "Smart-aggregation imaging for single molecule localisation with SPAD cameras," Scientific Reports 6 (2016).

[9] Gyongy, I., Davies, A., Gallinet, B., Dutton, N.A.W., Duncan, R., Rickman, C., Henderson, R.K., and Dalgarno, P., "Cylindrical microlensing for enhanced collection efficiency of small pixel SPAD arrays in single-molecule localisation microscopy," In Press: Optics Express (2018)

[10] Catipovic, M.A., Tyler, P.M., Trapani, J.G., and Carter, A.R., "Improving the quantification of Brownian motion," American Journal of Physics 81, 485-491, (2013).
[11] Smith, C.S., Joseph, N., Rieger, B., and Lidke, K.A., "Fast, single-molecule localization that achieves theoretically minimum uncertainty," Nature methods 7(5), 373-375 (2010).
[12] Gal, N., Lechtman-Goldstein, D., and Weihs, D., "Particle tracking in living cells: a review of the mean square displacement method and beyond," Rheol. Acta 52(5), 425–443 (2013).
[13] Michalet, X., "Mean square displacement analysis of single-particle trajectories with localization error: Brownian motion in an isotropic medium," Physical Review E 82(4), no. 4 (2010).
[14] Tinevez, J.-Y., Perry,N., Schindelin, J., Hoopes, G.M., Reynolds, G.D., Laplantine, E., Bednarek, S.Y., Shorte, S.L., and Eliceiri, K.W., "TrackMate: An open and extensible platform for single-particle tracking," Methods 115, 80-90 (2017).
[15] Rickman, C. and Duncan, R.R., "Munc18/Syntaxin Interaction Kinetics Control Secretory Vesicle Dynamics," Journal of Biological Chemistry 285(6), 3965-3972 (2010).
[16] Dun, A.R., Lord, G.J., Wilson, R.S., Kavanagh, D.M., Cialowicz, K.I., Sugita, S., Park, S., Yang, L., Smyth, A.M., Papadopulos, A. and Rickman, C., "Navigation through the Plasma Membrane Molecular Landscape Shapes Random Organelle Movement," Current Biology 27(3), 408-414 (2017).